Articles

The Role of Lysine 166 in the Mechanism of Mandelate Racemase from *Pseudomonas putida:* Mechanistic and Crystallographic Evidence for Stereospecific Alkylation by (*R*)-α-Phenylglycidate[†,‡]

James A. Landro,[§] John A. Gerlt,[*] and John W. Kozarich[*,∥]

Department of Chemistry and Biochemistry, University of Maryland, College Park, Maryland 20742

Carolyn W. Koo, Vibhakar J. Shah, and George L. Kenyon[*]

Department of Pharmaceutical Chemistry, University of California, San Francisco, California 94143

David J. Neidhart[*,⊥]

Monsanto Corporate Research, Mailzone BB4K, 700 Chesterfield Village Parkway, Chesterfield, Missouri 63198

Shigeo Fujita and Gregory A. Petsko[*]

Rosenstiel Basic Medical Sciences Research Center, Brandeis University, Waltham, Massachusetts 02254

Received July 15, 1993; Revised Manuscript Received September 23, 1993[⊛]

ABSTRACT: The mechanism of irreversible inactivation of mandelate racemase (MR) from *Pseudomonas putida* by α-phenylglycidate (αPGA) has been investigated stereochemically and crystallographically. The (*R*) and (*S*) enantiomers of αPGA were synthesized in high enantiomeric excess (81% ee and 83% ee, respectively) using Sharpless epoxidation chemistry. (*R*)-αPGA was determined to be a stereospecific and stoichiometric irreversible inactivator of MR. (*S*)-αPGA does not inactivate MR and appears to bind noncovalently to the active site of MR with less affinity than that of (*R*)-αPGA. The X-ray crystal structure (2.0-Å resolution) of MR inactivated by (*R*)-αPGA revealed the presence of a covalent adduct formed by nucleophilic attack of the ε-amino group of Lys 166 on the distal carbon of the epoxide ring of (*R*)-αPGA. The proximity of the α-proton of (*S*)-mandelate to Lys 166 [configurationally equivalent to (*R*)-αPGA] was corroborated by the crystal structure (2.1-Å resolution) of MR complexed with the substrate analog/competitive inhibitor, (*S*)-atrolactate [(*S*)-α-methylmandelate]. These results support the proposal that Lys 166 is the polyvalent acid/base responsible for proton transfers on the (*S*) face of mandelate. In addition, the high-resolution structures also provide insight into the probable interactions of mandelate with the essential Mg^{2+} and functional groups in the active site.

Mandelate racemase (MR)[1] (EC 5.1.2.2) from *Pseudomonas putida* ATCC 12633 catalyzes the interconversion of the (*R*) and (*S*) enantiomers of mandelic acid (Kenyon & Hegeman, 1979):

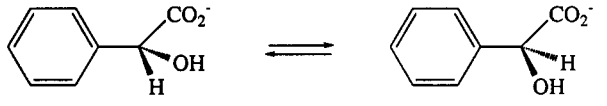

The enzyme is Mg^{2+}-dependent, and the reaction proceeds *via* abstraction of the α-proton from either enantiomer of mandelate followed by a stereorandom reprotonation of the stabilized enolic intermediate. Although the steady-state kinetic parameters of the racemization reveal bidirectional symmetry, a remarkable stereofacial asymmetry in the acid/base chemistry has been observed. Chemical and kinetic evidence has suggested the occurrence of two distinct acid/bases in the active site of MR: a monoprotic group effecting proton abstraction/addition from the (*R*) face of mandelate and a polyprotic group operating from the (*S*) face (Powers

[†] This research was supported by Grants GM-35066 (J.W.K.), GM-34572 (J.A.G.), and GM-40570 (J.A.G., G.L.K., J.W.K., and G.A.P.) from the National Institutes of Health. D.J.N. gratefully acknowledges the use of X-ray diffraction and computing equipment at Abbott Laboratories during his tenure on their staff.

[‡] Full atomic coordinates have been deposited with the Brookhaven Protein Data Bank under Accession Numbers 1MDR [mandelate racemase inactivated by (*R*)-α-phenylglycidate] and 1MNS [complex of mandelate racemase with (*S*)-atrolactate].

[§] This author was primarily responsible for the chemical and enzymological portions of the research described in this article. Present address: Department of Biology, Massachusetts Institute of Technology, Cambridge, MA 02139.

[∥] Present address: Department of Biochemistry, Merck Research Laboratories, P.O. Box 2000, Rahway, NJ 07065-0900.

[⊥] This author was primarily responsible for the structural portions of the research described in this article.

[⊛] Abstract published in *Advance ACS Abstracts,* November 15, 1993.

[1] Abbreviations: CD, circular dichroism; CAPS, 3-(cyclohexylamino)-1-propanesulfonic acid; CHES, 2-(cyclohexylamino)-1-ethanesulfonic acid; DCC, dicyclohexylcarbodiimide; DET, diethyl tartrate; DIBAL, diisobutylaluminum hydride; DMAP, 4-(dimethylamino)pyridine; FPLC, fast protein liquid chromatography; FTIR, Fourier-transformed infrared spectroscopy; H297N, the mutant of mandelate racemase in which the histidine at amino acid position 297 has been replaced with an asparagine; HEPES, 4-(2-hydroxyethyl)piperazine-1-ethanesulfonic acid; MES, 2-(*N*-morpholino)ethanesulfonic acid; MR, mandelate racemase; MS, mass spectroscopy; MTPA, α-methoxy-α-(trifluoromethyl)phenylacetic acid; NMR, nuclear magnetic resonance; αPGA, α-phenylglycidate; PIPES, piperazine-1,4-bis(2-ethanesulfonic acid); TAPS, *N*-[tris(hydroxymethyl)methyl]-3-aminopropanesulfonic acid; TBHP, *tert*-butyl hydroperoxide; TLC, thin-layer chromatography; TMS, trimethylsilane; Tris, tris(hydroxymethyl)aminomethane.

0006-2960/94/0433-635$04.50/0

Scheme I

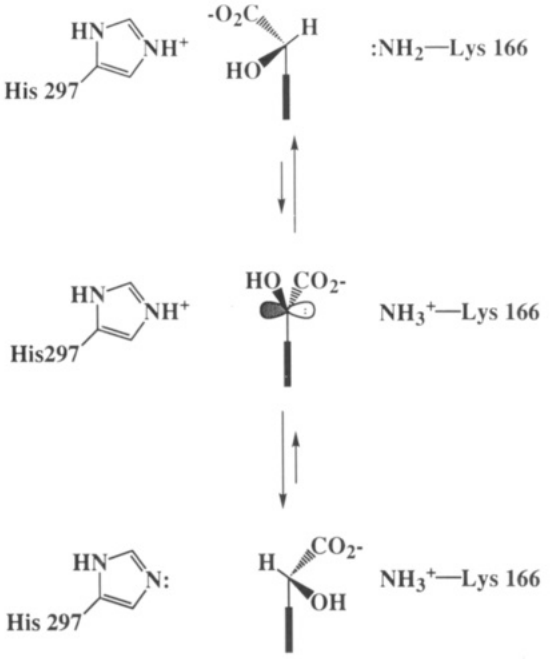

Scheme II

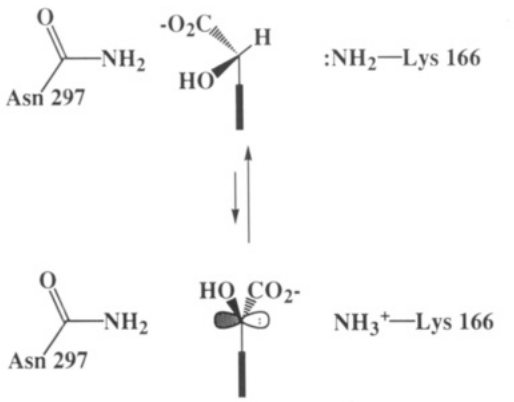

et al., 1991; Scheme I). A high-resolution X-ray structure of MR confirmed the active site asymmetry (Neidhart et al., 1991). On the basis of the positioning of a substrate analog, *p*-iodomandelate, in the crystal structure, the monoprotic acid/base was judged to be His 297 and the polyprotic acid/base to be Lys 166.

Evidence for the function of Lys 166 and His 297 was obtained from a mutant of MR in which His 297 was substituted with Asn (H297N). The high-resolution X-ray structure of H297N revealed no significant perturbation of the active site (Landro et al., 1991). Although inactive with respect to racemization, H297N catalyzed a stereospecific exchange of the α-proton of (*S*)-mandelate to afford (*S*)-[α-^{2}H]mandelate. The rate of the exchange was only 3-fold slower than the rate of racemization of mandelate by wild-type MR under comparable conditions (Landro et al., 1991). These observations are consistent with deprotonation of (*S*)-mandelate by Lys 166 to afford a stabilized, enolic intermediate that is sufficiently long-lived ($\geq 6.2 \times 10^{-10}$ s) to allow stereospecific delivery of a deuteron by rotation of the lysine ammonium ion as a minimal mechanism (Scheme II). In addition, the lack of racemization suggests that protonation of the intermediate from the (*R*) face (the His 297 side) is inhibited by the mutation to Asn, a considerably weaker acid than a His imidazolium ion. The pH–rate profile of proton exchange catalyzed by H297N suggested a pK_a of $\sim$6 for Lys 166 and permitted a calculation of the upper limit for the pK_a of the α-proton of enzyme-bound mandelate. The data were consistent with a pK_a of $\leq$14.6 for this proton. The assignment of Lys 166 as the acid/base was based on the X-ray structure, which placed it close to the α-proton (Neidhart et al., 1991). Glu 317 appeared positioned to donate a proton to the carboxylate group of mandelate, with Lys 164 and Mg^{2+} providing the charge neutralization that is essential for the activation of the α-proton and for the stabilization of the enolic intermediate.

In this article, we provide direct mechanistic and crystallographic evidence for the involvement of Lys 166 as the (*S*) face acid/base. We have reinvestigated the stereochemistry and stoichiometry of the inactivation of MR by the active site-directed epoxides (*R*)- and (*S*)-α-phenylglycidate (αPGA) prepared in high enantiomeric excess. Only (*R*)-αPGA inactivates MR to give a covalent adduct. The high-resolution X-ray structure of the adduct unambiguously establishes a covalent linkage between Lys 166 and the α-carbon of (*R*)-αPGA.

MATERIALS AND METHODS

Materials. All chemicals (Aldrich) used in synthetic procedures were reagent grade or better. Where indicated, solvents were dried using standard procedures. Thin-layer chromatography plates (silica, 0.02 × 20 × 20 cm) were purchased from Analtech. Silica used for flash chromatography (Universal Scientific, 40-μm "Flash") was purchased from Fisher Scientific.

General Methods. ^{1}H NMR spectra were recorded on a Brüker AM-200 (FT) or a Brüker AF-400 (FT) instrument. Chemical shifts were standardized to a HDO resonance at 4.7 ppm or a TMS resonance at 0.0 ppm in $CDCl_3$. Mass spectra were recorded on a VG 7070H spectrometer. IR spectra were recorded on a Nicolet 5DXC FT-IR spectrophotometer. Optical rotations were measured using a Jasco Model 370-DIP or a Perkin-Elmer Model 241 polarimeter.

Chemical Syntheses

Preparation and Analysis of Mosher Esters. Mosher esters of the enantiomeric phenyloxiranemethanols were prepared by the general method described by Nicolaou et al. (1989) and were used to assess enantiomeric purity. A stirred mixture of phenyloxiranemethanol (0.1 mmol), *R*-(+)-MTPA (0.17 mmol), DCC (0.17 mmol), and dry THF (1.0 mL) was treated with DMAP (0.05 mmol). The reaction mixture was stirred overnight, and the product ester was purified by preparative TLC. The enantiomeric purity was determined by ^{1}H NMR ($CDCl_3$, 400 MHz), which revealed the terminal methylene protons as AB doublets (δ 5.1–4.4 ppm).

Methyl 2-Phenyl-2-propenoate (**3**). A mixture of methyltriphenylphosphonium bromide (43 g, 120 mmol) and anhydrous THF (200 mL), in a dry 1-L round-bottom flask, was cooled to –23 °C under nitrogen, and *n*-butyllithium (75 mL, 120 mmol, 1.6 M in hexanes) was added dropwise over a period of 20 min. The solution was stirred (15 min), and methyl benzoylformate (16.4 g, 100 mmol) in 50 mL of THF was then added dropwise over a period of 20 min. The mixture was warmed to room temperature and stirred overnight. A solution of NH_4Cl [75 mL, 10% (w/v)] was added to the mixture, and the solution was extracted with Et_2O (3 × 100 mL). The organic layer was dried with $MgSO_4$, and solvent was removed under reduced pressure. Flash chromatography (30 mm diameter, 32 cm silica bed; 2:1 petroleum ether/

ether) yielded 9.2 g (57%) of the desired product (**3**) as an oil: IR (CCl_4) 3150, 3090, 3060, 2950, 1730, 1615, 1600, 1195, 1095, 908 cm^{-1}; ^1H NMR ($CDCl_3$, 400 MHz) δ 7.68–7.12 (m, 5), 6.35 (d, 1, J = 1.2 Hz), 5.87 (d, 1, J = 1.2 Hz), 3.8 (s, 3); mass spectrum, m/z (relative intensity) 162 (M^+, 28), 131 (12), 117 (15), 103 (100), 77 (49), 51 (35); exact mass, m/z 162.0680 (M^+), calcd for $C_{10}H_{10}O_2$, 162.0680.

2-Phenyl-2-propen-1-ol (**4**). A solution of anhydrous benzene (90 mL) and methyl 2-phenyl-2-propenoate (7.35 g, 45.7 mmol) in a 500-mL round-bottom flask was cooled to 0 °C under nitrogen. A DIBAL solution (95 mL, 95 mmol, 1 M in toluene) was added with a positive pressure of nitrogen over a period of 2.5 h. The reaction was stirred for an additional 16 h at room temperature. Excess DIBAL was quenched by cooling the reaction to 0 °C, followed by slow addition (20 min) of MeOH (150 mmol) in benzene (50 mL). The reaction mixture was transferred to a 1-L Erlenmeyer flask, and 50 mL of H_2O was added, whereupon a gel-like precipitate formed. The milky-white mixture was stirred vigorously for 45 min, filtered, and extracted with H_2O (2 × 60 mL). The organic layer was dried over $MgSO_4$, and the solvent was removed under reduced pressure. Flash chromatography (30 mm diameter, 31 cm silica bed, 2:1 petroleum ether/ether) afforded 3.92 g (65%) of pure **4** as an oil: IR (CCl_4) 3618, 3325, 3085, 3061, 3032, 2928, 2871, 1631, 1062, 908 cm^{-1}; ^1H NMR ($CDCl_3$, 400 MHz) δ 7.53–7.23 (m, 5), 5.47 (d, 1, J = 1.1 Hz), 4.55 (s, 2), 1.7 (s, 1); mass spectrum, m/z (relative intensity) 134 (M^+, 51), 133 (23), 105 (54), 103 (70), 92 (79), 91 (50), 78 (56), 77 (100), 51 (50); exact mass, m/z 134.0731 (M^+) calcd for $C_9H_{10}O$, 134.0731.

(2R)-Phenyloxiranemethanol (**5**). This compound was prepared by the general procedure for catalytic asymmetric epoxidation as described by Sharpless and co-workers (Gao et al., 1987). The reagents and conditions used were as follows: 30 mL of CH_2Cl_2 with 0.5 g of activated 4-Å molecular sieves, Ti(O-*i*-Pr)$_4$ (0.2 g, 0.7 mmol), D-(–)-DET (0.19 g, 0.9 mmol), 10.2 mL (3 M solution) of TBHP in isooctane (Aldrich) (30.6 mmol), and 2-phenyl-2-propen-1-ol (**4**, 2.05 g, 15.3 mmol) dissolved in 4 mL of CH_2Cl_2 (stored over 3-Å sieves), at an initial temperature of –23 °C. The reaction was stirred for 1 h at –23 °C and for 30 h at –20 °C. After workup B (Gao et al., 1987), the resulting oil was purified by flash chromatography (30 mm diameter, 17 cm silica bed, 1:1 petroleum ether/ether) to afford 1.83 g (80% yield, 83% ee determined by ^1H NMR analysis of the Mosher ester) of a colorless oil: $[\alpha]^{23}_D$ = +39.0° (c 0.3, $CHCl_3$); IR (CCl_4) 3580, 3450, 3060, 2960, 2920, 2870, 1500, 1450, 1370, 1150, 1090, 1040, 880, 860 cm^{-1}; ^1H NMR ($CDCl_3$, 200 MHz) δ 7.52–7.19 (m, 5), 4.1 (A of AB q, 1, J = 12.6 Hz), 3.99 (B of AB q, 1, J = 12.6 Hz) 3.26 (d, 1, J = 5.3 Hz) 2.81 (d, 1, J = 5.3 Hz); mass spectrum, m/z (relative intensity) 150 (M^+, 3), 149 (4), 133 (5), 120 (80), 105 (65), 91 (100), 77 (69), 65 (49), 51 (53); exact mass, m/z 150.0680 (M^+), calcd for $C_9H_{10}O_2$, 150.0680.

(2S)-Phenyloxiranemethanol (**6**). This compound was prepared in 76% yield (81% ee, determined by ^1H NMR analysis of the Mosher ester) by the same procedure used to prepare (*R*)-phenyloxiranemethanol (**5**), except that L-(+)-DET was used in place of D-(–)-DET. ($[\alpha]^{23}_D$ = –36.3° (c 0.33, $CHCl_3$)). The spectroscopic properties of this compound are identical to those of compound **5**.

Methyl (2R)-Phenyloxiranecarboxylate (**7**). This compound was prepared by a modification of the procedure of Sharpless and co-workers (Carlson et al., 1981). A 50-mL round-bottomed flask was charged with 5.4 mL of CH_3CN, 5.4 mL of CCl_4, 8 mL of H_2O, H_5IO_6 (1.92 g, 6.75 mmol), $NaHCO_3$ (1.14 g, 13.5 mmol), (2*S*)-phenyloxiranemethanol (**6**, 0.4 g, 3.4 mmol), and $RuCl_3{\cdot}xH_2O$ (13 mg, 0.06 mmol) and stirred with a magnetic stirrer for 24 h at room temperature. The reaction mixture was cooled to 4 °C, extracted with Et_2O (4 °C, 3 × 20 mL), dried over $MgSO_4$, reacted with ethereal diazomethane for 30 min, and concentrated under reduced pressure. The resulting oil was purified by thin-layer chromatography (Et_2O) to give a colorless oil in 71% yield: $[\alpha]^{21}_D$ = –26.5° (c 0.20, CCl_4); IR (CCl_4) 3040, 2950, 2930, 1750, 1730, 1450, 1315, 1280, 1180, 1110, 1060, 1030, 880, 840 cm^{-1}; ^1H NMR ($CDCl_3$, 200 MHz) δ 7.59–7.21 (m, 5), 3.79 (s, 3), 3.43 (d, 1, J = 6.3 Hz), 2.98 (d, 1, J = 6.3 Hz); mass spectrum, m/z (relative intensity) 178 (M^+, 12.8), 163 (7.1), 119 (13), 105 (100), 91 (49), 77 (42), 63 (12); exact mass, m/e 178.0628 (M^+), calcd for $C_{10}H_{10}O_3$, 178.0630.

Methyl (2S)-Phenyloxiranecarboxylate (**8**). This compound was prepared by the same procedure used to prepare **7**, except that (2*R*)-phenyloxiranemethanol (**5**) was used in place of (*S*)-phenyloxiranemethanol. A colorless oil was obtained in 74% yield ($[\alpha]^{21}_D$ = +27.2° (c 0.18, $CHCl_3$)). The spectroscopic properties of this compound are identical to those of compound **7**.

Potassium (2R)-Phenyloxiranecarboxylate ((R)-αPGA, 1). This compound was prepared by the saponification of methyl (2*R*)-phenyloxiranecarboxylate (**7**, 0.267 g, 1.5 mmol) with KOH (0.089 g, 1.59 mmol) in 30 mL of ethanol (95%) heated at reflux for 1.0 h. The solution was evaporated to dryness to yield a gummy solid. This solid was recrystallized from EtOH/Et_2O as a yellow solid in 38% yield: $[\alpha]^{21}_D$ = +30.1° (c 0.030, H_2O) (Whitman et al. (1985a) $[\alpha]^{21}_D$ = +41° (c 0.112, H_2O)); ^1H NMR (D_2O, 200 MHz) δ 7.38–7.3 (m, 5), 3.18 (AB q, 2, J = 4.9, 12.6 Hz).

Potassium (2S)-Phenyloxiranecarboxylate ((S)-αPGA, 2). This compound was prepared by the same procedure used to prepare **1**, except that methyl (2*S*)-phenyloxiranecarboxylate (**8**) was used in place of methyl (2*R*)-phenyloxiranecarboxylate (**7**). A yellow solid was obtained in 33% yield: [a]$^{21}_D$ = –28.6° (c 0.035, H_2O) (Whitman et al. (1985a) $[\alpha]^{21}_D$ = –26° (c 0.116, H_2O)). The ^1H NMR spectrum of this compound is identical to that of compound **1**.

(R)-(–)-Atrolactic Acid and (S)-(+)-Atrolactic Acid. Both enantiomers of atrolactic acid (2-hydroxy-2-phenylpropionic acid) were purchased from Lancaster Synthesis Inc. as 97% pure compounds. Each enantiomer was repetitively crystallized from hot benzene until a constant specific rotation was achieved. The enantiomeric excess was determined by chromatographic analysis on a Regis Chiralcel column at 4 °C (95:5:0.1 *n*-hexane/isopropyl alcohol/trifluoroacetic acid, 0.5 mL/min). (*R*)-Atrolactate: retention time, 23 min; 99% ee; $[\alpha]^{23}_D$ = –36.25° (c 1.68, EtOH). (*S*)-Atrolactate: retention time, 28 min; 99% ee; $[\alpha]^{23}_D$ = +36.46° (c 1.67, EtOH).

Enzymological Methods

Enzyme Purification. Wild-type mandelate racemase (MR) was expressed in *E. coli* and purified by the method of Tsou et al. (1989). The specific activity was 1010 units/mg (k_{cat} ≈700 s^{-1}; 39 000 Da/monomer), as determined by the circular dichroic assay (Sharp et al., 1979) in 100 mM HEPES (pH 7.5) containing 5 mM (*R*)-mandelate and 3 mM $MgCl_2$, at 25 °C using a Jasco J-500C spectropolarimeter. The concentration of the stock solution of enzyme was determined

using the microbiuret assay (Bailey, 1962) with bovine serum albumin (Sigma) as a standard.

Kinetics of Irreversible Inhibition. The inhibition of MR with the enantiomeric αPGAs was carried out according to the protocol of Kenyon and co-workers (Fee et al., 1974) with the following modifications. Residual MR activity was monitored by the circular dichroic assay in 100 mM HEPES (pH 7.5) containing 3 mM $MgCl_2$ as described above. This buffer was also used for enzyme inactivation. Activity assays were initiated by the addition of (*R*)-mandelate to give a final concentration of 5 mM. The concentration of inactivator used in these studies was determined by CD spectroscopy (Jasco J-500C spectropolarimeter equipped with a Jasco DP-500N data processor) using the measured molar ellipticities in H_2O: (*R*)-αPGA, $\theta = +1900$ deg cm^2 dmol^{-1} (205 nm); (*S*)-αPGA, $\theta = -1955$ deg cm^2 dmol^{-1} (205 nm).

The dependence of k_i and K_I on pH with (*R*)-αPGA was evaluated in 100 mM buffers, pH 5.5–10.0, containing 10 mM $MgCl_2$. The buffers used were as follows: MES, pH 5.5, 6.0; PIPES, pH 6.5, 7.0; HEPES, pH 7.5, 8.0; TAPS pH 8.5, 9.0; CHES, pH 9.0, 9.5; and CAPS, pH 10.0. As shown earlier (Landro et al., 1991), MR was stable for moderate periods of time at the pH extremes investigated. The use of overlapping pH ranges in that study ensured that no discontinuities or artifacts resulted from the use of six different buffers across the pH range examined. The stability of (*R*)-αPGA at the pH extremes was verified by monitoring the ^1H NMR spectrum as a function of time in MES and CAPS buffers (pD 5.5 and 10.0, respectively). The spectra displayed no changes after 30 min.

Kinetic Analysis of Reversible Inhibition of Mandelate Racemase by (S)- and (R)-Atrolactates. The K_i's of (*S*)- and (*R*)-atrolactates for both the *S* to *R and R* to *S* directions were determined by the circular dichroic assay (Sharp et al., 1979). Assays (12.5 mL) were performed at 25 °C in a 5-cm quartz cell in 50 mM MES (pH 6.0) containing 3 mM $MgCl_2$ and varying concentrations of the enantiomers of mandelate (0.5, 1.0, and 2.0 mM) and atrolactate (0, 0.25, 0.5, 1.0, and 2.0 mM). The data were fit to the equation for competitive inhibition using KinetAsyst software (IntelliKinetics, State College, PA).

Stoichiometry of Inactivation of Mandelate Racemase in the Presence of (R)- and (S)-α-Phenylglycidate. The efficacy of both (*R*)- and (*S*)-αPGA as inactivators of MR was determined by comparing the residual MR activity as a function of time in the presence of a stoichiometric amount of each enantiomer. MR (13.5 mg/mL stock solution, determined by the microbiuret assay) was diluted to 1 mL (final concentration 2.5 mg/mL, 64 μM) in HEPES/Mg buffer containing either (*R*)- or (*S*)-αPGA (64 μM, determined by molar ellipticity). The residual activity of a small aliquot of these reactions was measured using the CD assay.

Preparation of Mandelate Racemase Inactivated by (R)-α-Phenylglycidate. Inactivated mandelate racemase for crystallographic studies was prepared by the incubation of (*R*)-αPGA (1 mM, ~10–20 K_I) with ~3 mg of MR until the remaining racemase activity was <0.5% (~2 days). Inactivator and inactivated enzyme were separated from one another using a Pharmacia FPLC system equipped with a Superose 12 column equilibrated with 100 mM Tris-HCl/3.0 mM $MgCl_2$ buffer.

Structural Determination Methods

Crystallization. For crystallization, the αPGA-inactivated enzyme was dialyzed into 50 mM Tris buffer (pH 8.0) containing 10 mM $MgCl_2$ and concentrated to about 3 mg/mL. Crystals were grown from aqueous ammonium sulfate using methods previously described for native mandelate racemase (Neidhart et al., 1991) and were isomorphous with native mandelate racemase crystals, with cell dimensions $a = b = 125.0$ Å and $c = 105.6$ Å and space group *I*422.

Cocrystallization of MR with (*S*)-atrolactate was achieved as follows. (*S*)-Atrolactic acid (Aldrich) was added, to a final concentration of 3 mM, to a 25% saturated solution of aqueous ammonium sulfate. This solution was neutralized by the addition of sodium hydroxide and then mixed with enzyme solution (3 mg/mL in 50 mM Tris buffer (pH 8.0) containing 10 mM $MgCl_2$) in a standard hanging-drop vapor diffusion format. These crystals were also isomorphous with native mandelate racemase crystals, with cell dimensions $a = b = 125.2$ Å and $c = 105.7$ Å and space group *I*422.

X-ray Data Collection. For MR inactivated by (*R*)-αPGA, diffraction data to 2.0-Å resolution were collected from a single crystal of inactivated MR using a Siemens multiwire area detector installed on a Rigaku RU200 rotating anode X-ray generator. The generator was operated at 5 kW (50 kV × 100 mA) with a 0.3 × 3 mm focal spot at the anode. The crystal dimensions were about 0.6 × 0.4 × 0.3 mm, but Frank's mirrors were used to produce a collimated beam width of about 0.2 mm at the crystal. An additional filter of 0.020-in. nickel foil served to attenuate and further monochromate the X-ray beam. A single sweep of diffraction data comprising a 115° rotation was collected as a set of 460 frames of 0.25° each at a crystal-to-detector distance of 14 cm and a 2Θ offset of 25 °C. The exposure time for each frame image was 2 min, and about 2 million photon counts were accumulated for each frame. The data set is 92% complete to 2.0-Å resolution, with about 50% of the data observed ($>1\sigma(F)$) in the 2.3–2.0-Å shell. The $R_{sym}(F)$ for data greater than $1\sigma(F)$ to 2.0 Å is 7.5% after spherical harmonic scaling and rejection of 2174 observations out of 62 094 collected. All scaling and rejection were performed with the Xengen package (Howard, 1990).

For MR cocrystallized with (*S*)-atrolactate, diffraction data were collected to 2.1 Å using conditions similar to those described above. Two sweeps of diffraction data were collected as sets of 360 frames. The data set is 85% complete to 2.1-Å resolution, with about 50% of the data observed ($>1\sigma(F)$) in the 2.3–2.0-Å shell. The $R_{sym}(F)$ for data greater than $1\sigma(F)$ to 2.0 Å is 8.1% after spherical harmonic scaling and rejection of 9974 observations out of 89 227 collected.

Statistics on the data sets are summarized in Table I.

Structure Solution and Refinement. The crystal structures were solved by difference Fourier analyses relative to the highly refined ($R = 16.3\%$) 2.0-Å structure of the native enzyme (D. J. Neidhart, unpublished results). The structures were then refined against X-ray diffraction data to the usable resolutions of the X-ray data sets using energy refinement as implemented in XPLOR (Brünger et al., 1987). Energetic parameters for inhibitors were selected from the XPLOR and CHARMM param19 parameter sets or derived by analogy to existing parameters in those sets. Rigid-body minimization followed by several cycles of energy-based positional refinement, restrained individual isotropic *B* factor refinement, and manual rebuilding reduced the *R* factor from initial values of about 20% to 15.3% for the enzyme inactivated with α-phenylglycidate and to 15.1% for the complex with the substrate analog. In each structure, approximately 200 water molecules are included per 38 570-Da subunit, four of which lie on 2-fold axes of symmetry within the 422 octameric structure. Statistics on the refinements are summarized in Table II.

Table I: Diffraction Data Statistics[a]

data set	MR + (R)-αPGA[b]	MP + (S)-atrol[c]
cell dimensions (Å)	$a = B = 125.0$ $c = 105.6$	$a = b = 125.2$ $c = 105.7$
nominal resolution (Å)	2.0	2.1
2θ offset (deg)	25	25
camera length (cm)	14	14
frame width on ω (deg)	0.25	0.25
no. of sweeps	1	2
no. of frames/sweep	460	360
exposure time/frame (min)	2	2
no. of counts/frame (million)	2	2
R-merge[d] (%)	7.5	8.1
completeness[e] (%)	83 (47)	85 (63)
total observations	62094	89227
observations rejected in scaling	2174	9974
redundancy	2.6	3.7

[a] All processing of Siemen's X-ray area detector data was performed with use of the XENGEN suite of programs (Howard, 1990). [b] MR inactivated with (R)-αPGA. [c] Complex of MR with (S)-atrolactate. [d] R-merge = $\Sigma|I(k) - \langle I\rangle|/\Sigma I(k)$, where $I(k)$ represents the intensity of an individual observation and $\langle I\rangle$ is the mean of the related observations corresponding to a unique reflection k. Observations with $I/\sigma(I) < 1.0$ were excluded from all calculations. [e] Percent of theoretically possible reflections observed with $I/\sigma(I) \geq 1.0$ and with the outermost shell of width 0.1-Å resolution in parentheses.

Table II: Refinement Statistics[a]

structure	MR + (R)-αPGA[b]	MR + (S)-atrol[c]
nominal resolution (Å)	2.0	2.1
no. of reflections[d]	22159	18059
no. of protein atoms[e]	2698	2698
no. of inhibitor atoms	12	12
metal ions	1 Mg^{2+}	1 Mg^{2+}
no. of water molecules	209	207
deviation in bond distances[f] (Å)	0.015	0.016
deviation in bond angles[f] (deg)	2.6	2.8
deviation in dihedral angles[f] (deg)	23.4	23.7
deviation in improper torsions[f] (deg)	1.2	1.3
R factor[g]	0.153	0.151

[a] Refinement was performed with the XPLOR package (Brünger et al., 1987). [b] MR inactivated with (R)-αPGA. [c] Complex of MR with (S)-atrolactate. [d] Reflections used in refinement have $I \geq \sigma(I)$ and resolutions between 6.0 Å and the indicated nominal resolution of the data set. [e] This is the number of non-hydrogen atoms in the final model, excluding water, metal ion, and sulfate or inhibitor atoms; polar hydrogens are introduced during XPLOR refinement to facilitate energetic modeling of hydrogen bonds but are excluded from X-ray structure factor calculations and are not included in the reported X-ray structure. [f] These values are root-mean-square deviations from the "ideal" values in the XPLOR param19x.pro parameter set. [g] The R factor is calculated using all data with $I \geq \sigma(I)$ from 6.0 Å to the specified nominal resolution.

Both structures have been deposited in the Protein Data Bank at Brookhaven National Laboratories.

RESULTS AND DISCUSSION

Enantioselective Synthesis of (R)- and (S)-αPGAs. The chemical syntheses of (R)- and (S)-αPGAs (**1** and **2**, respectively) are shown in Scheme III. The key step is the epoxidation of compound **4** with high enantioselectivity using catalytic asymmetric epoxidation (Gao et al., 1987). The enantiomeric content of the initially formed epoxides, **5** and **6**, was used to establish the enantiomeric content of (R)- and (S)-αPGA (**1** and **2**), respectively. Thus, the enantiomeric excess (ee) of (R)-αPGA and of (S)-αPGA was determined to 83% and 81%, respectively. A previous study used αPGAs that were enantiomerically enriched by a resolution of the diastereomeric (–)-2-octyl ester derivatives (Whitman et al., 1985a,b). This procedure afforded (R)-αPGA of 56% ee and (S)-αPGA of 34% ee. Asymmetric epoxidation, then, represents a considerable improvement over the previous method of chiral resolution.

Scheme III[a]

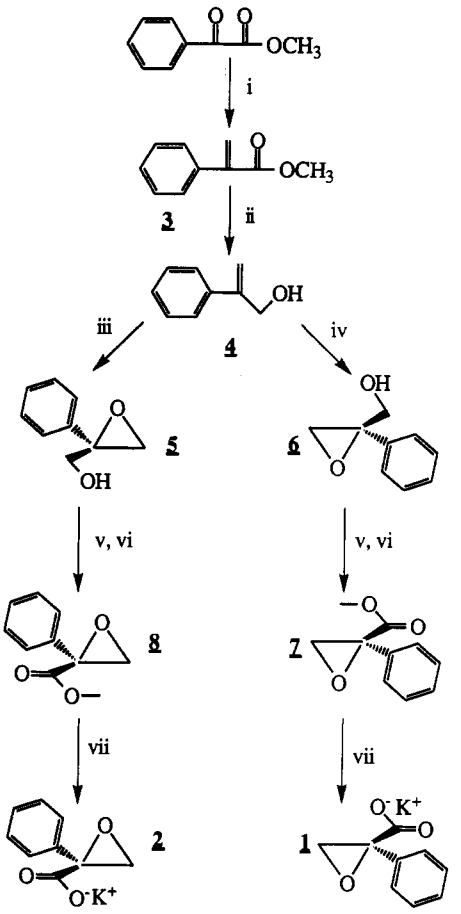

[a] (i) n-BuLi/$[(Ph_3P)_3Me^+]Br^-$; (ii) DIBAL, 0 °C; (iii) Sharpless epoxidation, D-(–)-DET; (iv) Sharpless epoxidation, L-(+)-DET; (v) $NaHCO_3$, H_5IO_6, $RuCl_3$, $CH_3CN/CCl_4/H_2O$;(vi) CH_2N_2; (vii) KOH/95% EtOH.

Time-Dependent Inactivation of Mandelate Racemase with (R)- and (S)-α-Phenylglycidates. Enantiomerically enriched preparations of both (R)- and (S)-αPGA caused time-dependent, irreversible inactivations of mandelate racemase by a first-order process (Figures 1A,B). The values of $t_{1/2}$ obtained from these plots were used to calculate k_{inact} for each concentration used. A plot of $1/k_{inact}$ *vs* $1/[I]$ for each enantiomer is shown in Figure 2. The values of k_{inact} and K_I obtained from this plot for (R)-αPGA are 0.011 ± 0.005 s^{-1} and 67 ± 44 μM, respectively, while the values obtained for (S)-αPGA are 0.007 ± 0.002 s^{-1} and 112 ± 45 μM. The data indicate that the inactivation obeys saturation kinetics and, therefore, occurs *via* an enzyme·αPGA complex. The results strongly suggest that, at a minimum, (R)-αPGA is the more potent inactivator of MR. This conclusion is consistent with earlier studies using racemic and partially resolved αPGAs, although our kinetic parameters differ (Fee et al., 1974; Whitman et al., 1985b). We attribute the differences to the substantial improvement in the enantiomeric content of the αPGAs and recent refinements in the production of substantial amounts of recombinant MR with high specific activity (Tsou et al., 1989).

Two questions that cannot be definitively answered by the inactivation kinetics are the following: (1) Is (S)-αPGA a competitive inhibitor of inactivation of MR by (R)-αPGA and of racemization of mandelate? (2) Is (S)-αPGA an inactivator of MR albeit less potent than (R)-αPGA? Since

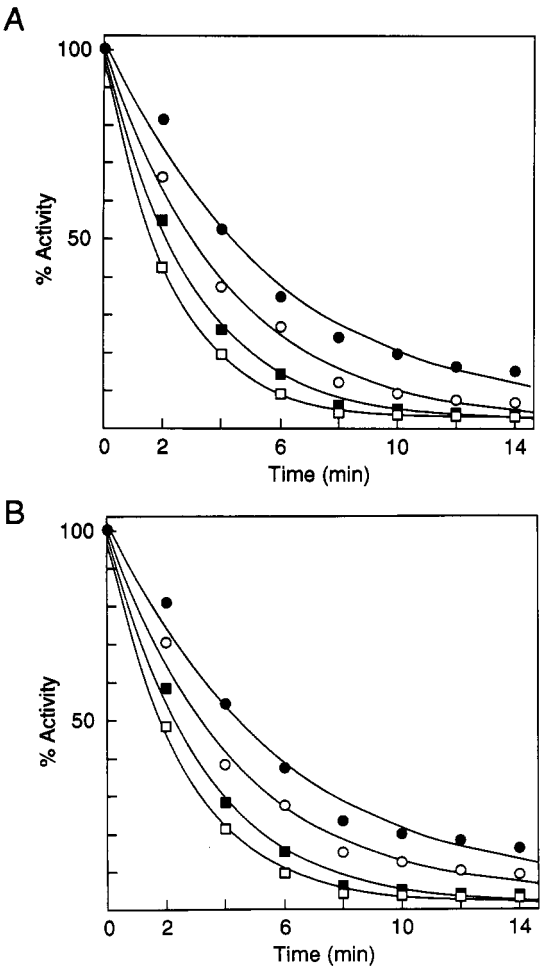

FIGURE 1: (A) Time course of the inactivation of MR by (*R*)-αPGA: 10 (●); 20 (○); 30 (■); 40 μM (□). (B) Time course of the inactivation of MR by (*S*)-αPGA: 30 (●); 60 (○); 90 (■); 120 μM (□). Data points were fit to a first-order equation by a nonlinear regression analysis.

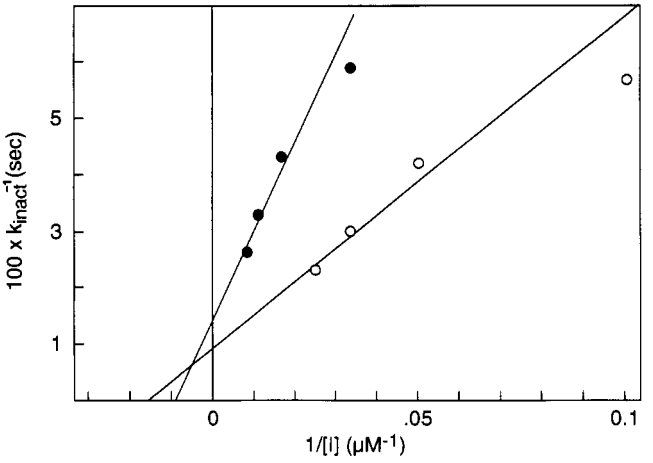

FIGURE 2: Double-reciprocal plot of the observed values for k_{inact} *vs* concentration: (*R*)-αPGA, (○); (*S*)-αPGA (●). Data points were fit to a linear equation by a nonlinear regression analysis.

(*S*)-αPGA is contaminated by a significant amount of (*R*)-αPGA (~10%), the inactivation of MR by (*R*)-αPGA, which is in excess over enzyme, complicates the analysis of the mode of inhibition by (*S*)-αPGA. Our results do suggest that, if (*S*)-αPGA binds to MR competitively, it is a weaker inhibitor than (*R*)-αPGA. This is best understood by considering the extreme case where (*S*)-αPGA does not bind to MR. Under these conditions, the k_{inact}'s for both enantiomerically enriched (*R*)- and (*S*)-αPGAs would be identical since k_{inact} would be determined solely by (*R*)-αPGA; however, the K_I's would reflect the content of (*R*)-αPGA in each preparation. Alternatively, if (*S*)-αPGA competes with (*R*)-αPGA for binding to MR, then both k_{inact} and K_I will be sensitive to the enantiomeric content of the (*S*)-αPGA. The similar k_{inact}'s and higher K_I for (*S*)-αPGA suggests that (*S*)-αPGA is, within the errors of the experimental procedure, a weaker binder than (*R*)-αPGA.

Table III: Stoichiometry of Inactivation of MR by (*R*)- and (*S*)-αPGAs[a]

isomer	% ee[b]	nmol of (*R*) isomer added[c]	nmol of inactive enzyme[d,e]	% inactivation
(*R*)-αPGA	81	58	52	81
(*S*)-αPGA	83	6	17	26

[a] Separate aliquots of MR (64 nmol in 1 mL of 100 mM HEPES (pH 7.5)) and 3 mM $MgCl_2$ were inactivated with an equimolar amount of each isomer. The residual enzyme activity relative to an untreated control was monitored by the CD assay over a 48-h period at 25 °C (see Materials and Methods). [b] Determined by ^1H NMR analysis of the Mosher esters of **5** and **6** (see Materials and Methods). [c] Of enantiomer corrected for % ee. [d] Based on a specific activity of 1010 units/mg for MR. [e] Values are the average of two determinations and represent the activity remaining after 48 h.

In order to probe further the relative binding of the enantiomers in the absence of inactivation, (*R*)- and (*S*)-atrolactates (α-methylmandelates) were resolved (>99% ee) and evaluated as reversible inhibitors of the racemase. The atrolactates are structurally related to the αPGAs and may be viewed as analogs of the epoxide-opened form. Both (*R*)- and (*S*)-atrolactates were found to be competitive inhibitors of MR. Using (*R*)-mandelate as substrate, the K_I's for (*R*)- and (*S*)-atrolactates are 0.41 ± 0.03 and 0.14 ± 0.02 mM, respectively. Using (*S*)-mandelate as substrate, the K_I's for (*R*)- and (*S*)-atrolactates are 0.30 ± 0.04 and 0.15 ± 0.03 mM, respectively. Thus, (*S*)-atrolactate binds somewhat more strongly to the active site than (*R*)-atrolactate. Since (*R*)-atrolactate is configurationally equivalent to (*S*)-αPGA, i.e., the α-methyl group and the unsubstituted methylene group of the oxirane ring are expected to occupy the same region of the active site, these data are in qualitative accord with the conclusion that (*R*)-αPGA binds to the active site more strongly than (*S*)-αPGA.

In order to determine whether (*S*)-αPGA is an irreversible inactivator of the racemase, a different experimental approach was used. For the kinetic studies discussed above, the αPGAs were in large excess over the concentration of enzyme. Therefore, if one isomer were a more potent inactivator than the other [as the (*R*)-αPGA appears to be], an impurity of this isomer in the preparation of its enantiomer would cause the kinetics of inactivation to appear as though both isomers were effective inactivators. This is consistent with the kinetics observed. We tested this possibility by monitoring the inactivation of the racemase using an equimolar amount of either (*R*)- or (*S*)-αPGA (64 μM) with respect to active site concentration. As shown in Table III, in the presence of (*R*)-αPGA, the enzyme loses ~ 80% of its initial activity within an hour and the remaining level of activity is stable for several days. In the presence of (*S*)-αPGA, the loss in enzyme activity remains constant at ~25%. Under conditions of 1:1 stoichiometry, therefore, the extent of inactivation of the racemase approximates the enantiomeric content of the (*R*)-αPGA. These results suggest that only (*R*)-αPGA is capable of inactivating MR. Errors in the measurement of ee and/or protein content most likely account for the deviation from the

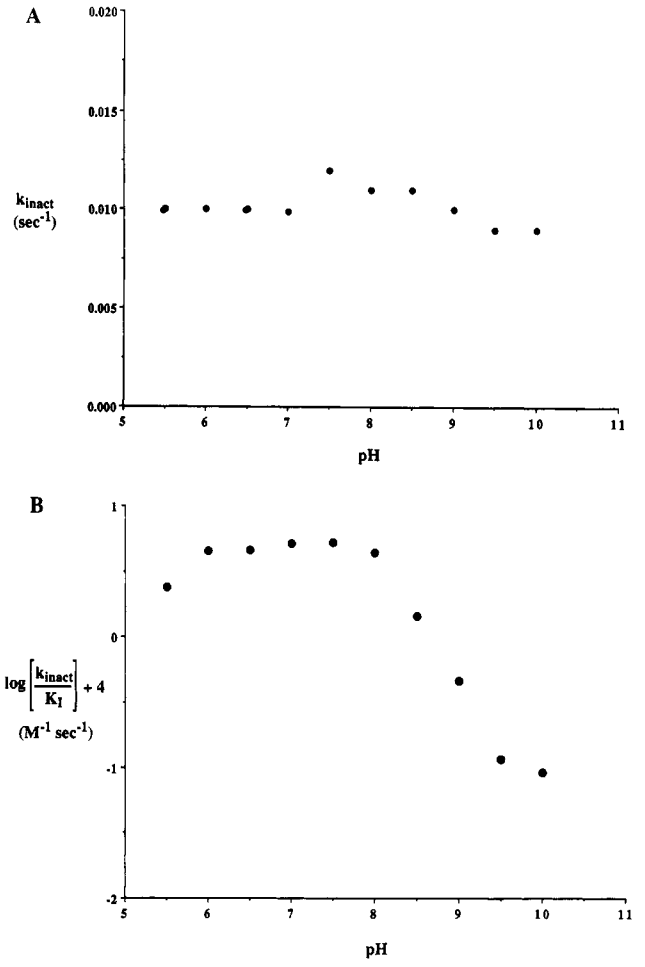

FIGURE 3: (A) Dependence of k_{inact} for (*R*)-αPGA on pH. (B) Dependence of k_{inact}/K_I for (*R*)-αPGA on pH.

predicted extents of inactivation. The inequality of inactivation we have observed for the enantiomeric α-phenylglycidates is in contrast to previous studies performed by Kenyon and coworkers (Whitman et al., 1985b) with the structurally similar compounds, (*R*)- and (*S*)-α-phenylglycerate (2,3-hydroxy-2-phenylpropionic acid). It was observed that these compounds reversibly inhibited mandelate racemase with nearly equal affinities, with the value of K_i being ≈1.3 mM.

Kinetics of Inactivation of Mandelate Racemase As a Function of pH. Previous studies investigating the dependence of k_{cat} on pH suggested that, in both the *R* to *S* and *S* to *R* directions, the pK_a values assigned to the active site bases Lys 166 and His 297 are 6.4 and 10.0. This prompted us to investigate the kinetics of inactivation of MR with (*R*)-αPGA as a function of pH. It is reasonable to predict that the MR-catalyzed opening of the epoxide ring is achieved by protonation of the epoxide oxygen atom by the active site general acid concomitant with nucleophilic attack by the active site general base at C-3. Therefore, at low pH (5.5), the active site base is expected to be protonated, which should decrease its nucleophilicity, while the acid residue will not be affected; at high pH (10.0) the active site acid will be deprotonated, which will decrease its effectiveness as a general-acid catalyst while the nucleophilicity of the general base should be unimpeded. As shown in Figure 3A, in contrast to the dependency of k_{cat} on pH, the magnitude of k_{inact} appears to be pH-independent over the range investigated (5.5–10.0). However, it is clear from Figure 3B that the magnitude of K_I increases as the pH is increased above 8.0. It is not clear why the active site residues Lys 166 (nucleophile) and His 297 (general acid) participating

Scheme IV

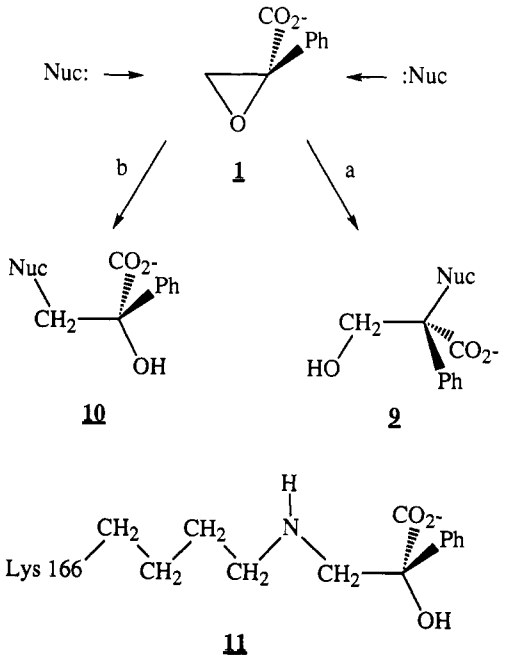

in the epoxide opening reaction are not titratable with respect to k_{inact}. It should be noted that the H297N mutant of MR (Landro et al., 1991) is not inactivated by either enantiomer of αPGA under conditions which lead to >99% inactivation of wild-type MR (J. A. Landro and J. W. Kozarich, unpublished data). This would suggest that Asn 297 is incapable of functioning as a general-acid catalyst in epoxide protonation in accord with its inability to protonate the enzyme intermediate resulting from Lys 166 deprotonation of (*S*)-mandelate.

Chemical Structure of the Adduct. The epoxide ring of (*R*)-αPGA (**1**) is subject to nucleophilic attack at either of two carbon atoms to yield distinct products. Attack at the α-carbon of **1** (Scheme IV, path a) will yield **9**, whereas attack at the distal endocyclic carbon atom (Scheme IV, path b) will produce **10**. The crystal structure of the inactivated complex obtained by incubation of(*R*)-αPGA with MR (Figure 4, yellow structure) reveals that an adduct consistent with the structure of **10** is formed by nucleophilic attack of the Lys 166 side-chain ε-amino group on the distal carbon of the epoxide ring (**11**). Although epoxides frequently react by nucleophilic substitution at the more electrophilic (i.e., more substituted) carbon atom of the oxirane ring, the reaction of the Lys 166 ε-amino group with the inactivator is restrained by the geometry of the active site. In fact, αPGA was originally designed as a mechanistic probe of mandelate racemase on the premise that the distal oxirane carbon occupies a position similar to that of the α-proton in mandelate (Fee et al., 1974). Thus, upon binding of the inactivator to the active site of the enzyme, this electrophilic group would be subject to attack by the active site basic group responsible for abstraction of the α-proton in the normal catalytic cycle (Scheme I). The observed structure of the (*R*)-αPGA adduct with MR validates this design strategy and suggests that, despite its function as a randomizer of stereochemistry, mandelate racemase is exquisitely sensitive to the geometry of bound ligands. Moreover, the structure strongly implicates Lys 166 as the active site base responsible for α-proton abstraction from (*S*)-mandelate. This is consistent with the conclusions drawn from the previously reported crystal structure (Neidhart et al., 1991). This point is further corroborated by the X-ray

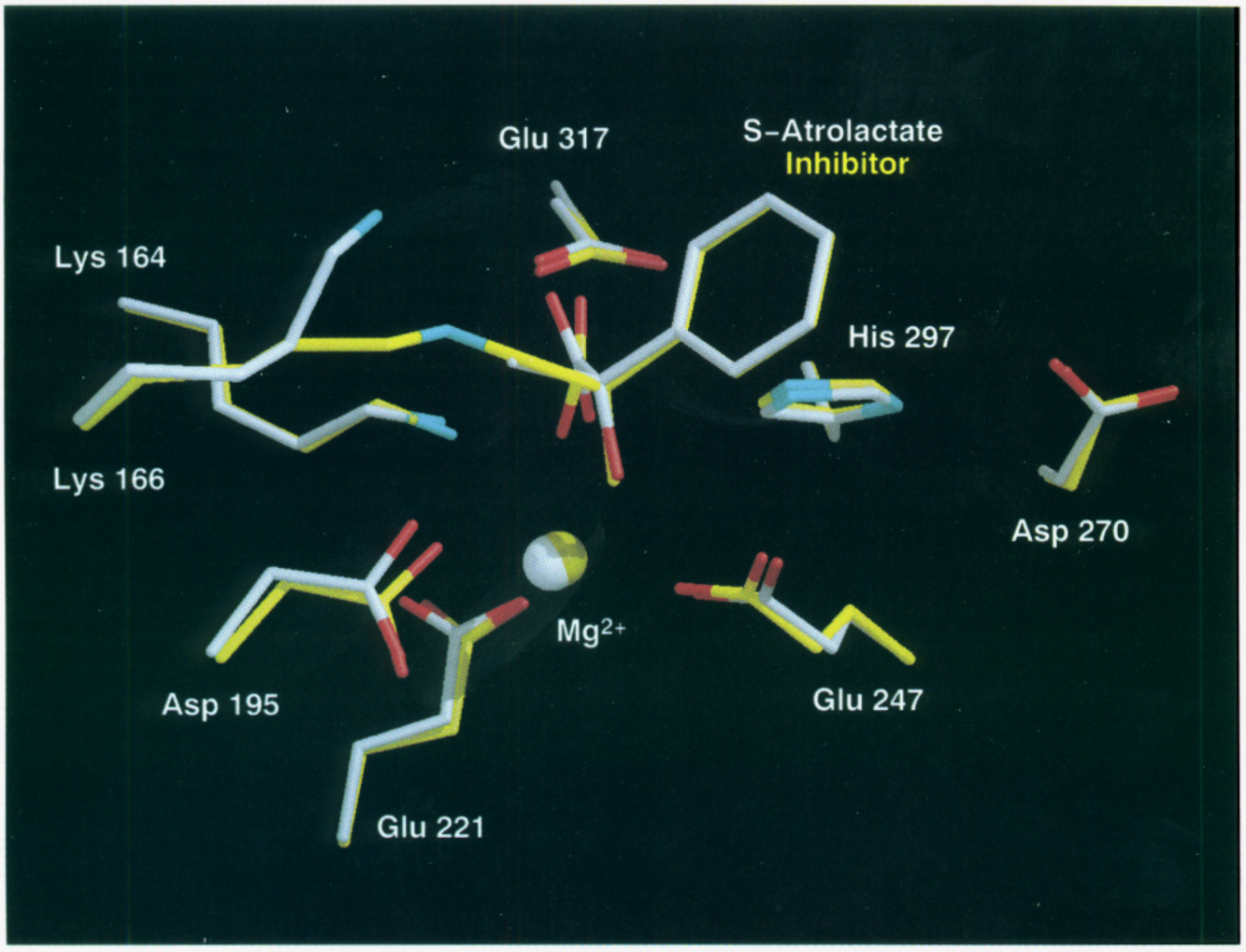

FIGURE 4: Superposition of the X-ray structures of the active site of MR inactivated by (*R*)-αPGA (yellow) and of the active site of MR with (*S*)-atrolactate bound in the active site (white). The epoxide ring of the inhibitor alkylated the ϵ-amino group of Lys 166.

structure of (*S*)-atrolactate bound to the racemase (Figure 4, white structure). The structure reveals a displacement of Lys 166 away from the α-methyl group of (*S*)-atrolactate [positionally equivalent to but larger than the α-proton in (*S*)-mandelate] while the remaining active site residues show negligible perturbation.

Interactions of Substrate Analogs with the Active Site. Both high-resolution crystal structures (Figure 4) permit detailed analyses of the interactions of the substrate analogs with the enzyme. Since it has proved difficult to determine the structures of complexes between MR and the enantiomers of mandelate, the structures of these complexes provide mechanistically valuable insight into the geometry of the interaction of (*S*)-mandelate with functional groups at the active site. Since (*S*)-αPGA fails to form a covalent adduct with MR, and (*R*)-atrolactate fails to bind in a unique geometry to the active site (J. A. Landro, J. W. Kozarich, J. R. Clifton, and G. A. Petsko, unpublished results), the exact mode of interaction of (*R*)-mandelate with MR remains uncertain, although we presume it to be similar to that which we describe herein.

Both substrate analogs are coordinated to the catalytically essential Mg^{2+} through the α-hydroxyl oxygen and one of the carboxylate oxygens. These structures provide the first direct evidence that analogs of mandelate can form chelates with the divalent metal ion at the active site of MR. That these chelates also involve metal–hydroxyl oxygen coordination provides an explanation for the fact that MR fails to catalyze exchange of the α-protons of either phenylacetate or α-fluorophenylacetate with solvent (V. M. Powers, Judith A. Fee, and G. L. Kenyon, unpublished results).

In addition, both carboxylate oxygens of the substrate analogs are in appropriate positions and orientations to form hydrogen bonds with polar atoms in the active site. In both structures, the carboxylate oxygen of the substrate analog that is coordinated to the metal ion is also hydrogen-bonded to the ϵ-ammonium group of Lys 164. These interactions should neutralize the negative charge of the carboxylate group of bound mandelate, thereby allowing the bound substrate to react as if its electronic character resembled that of a neutral carboxylic acid rather than a carboxylate anion. In both structures, the short distance between the other carboxylate oxygen of the substrate analog and the γ-carboxyl group of Glu 317 (~2.7 Å) indicates that the side-chain carboxyl group is protonated. With this hydrogen bond, Glu 317 would be able to serve as a general-acid catalyst, thereby explaining the remarkable drop in pK_a of the α-proton from its value of about 22 for mandelic acid in aqueous solution (Chiang et al., 1990) to the value of ≤14.6 required to rationalize the observed rate of α-proton solvent exchange in the H297N mutant of mandelate racemase (Landro et al., 1991; Gerlt et al., 1991; Gerlt & Gassman, 1993).

Conclusions. The nature of the inactivation of MR by α-PGA has been elucidated by a combination of stereospecific synthesis and X-ray crystallography. The ϵ-amino group of Lys 166, one of the putative acid/base catalysts, is alkylated

by (*R*)-αPGA. The structure of this inactivated complex, as well as that of the competitive inhibitor (*S*)-atrolactate, bound in the active site reveals the probable interactions of substrate mandelate with the essential Mg^{2+} and active site functional groups.

REFERENCES

Bailey, J. L. (1962) in *Techniques in Protein Chemistry*, p 294, Elsevier, New York.

Brünger, A. T., Kuriyan, J., & Karplus, M. (1987) *Science 235*, 458–460.

Carlson, P. H. J., Katsuki, T., Martin, V. S., & Sharpless, K. B. (1981) *J. Org. Chem. 46*, 3936–3638.

Chiang, Y., Kresge, A. J., Pruszynski, P., Schepp, N. P., Wirz, J. (1990) *Angew. Chem., Int. Ed. Engl. 29*, 792–794.

Fee, J. A., Hegeman, G. D., & Kenyon, G. L. (1974) *Biochemistry 13*, 2533–2538.

Gao, Y., Hanson, R. M., Klunder, J. M., Soo, Y. K., Masamune, H., & Sharpless, K. B. (1987) *J. Am. Chem. Soc. 109*, 5765–5780.

Gerlt, J. A., & Gassman, P. G. (1993) *J. Am. Chem. Soc.* (in press).

Gerlt, J. A., Kozarich, J. W., Kenyon, G. L., & Gassman, P. G. (1991) *J. Am. Chem. Soc. 113*, 9667–9669.

Howard, A. J. (1990) *A Guide to Macromolecular X-ray Data Reduction for the Siemens Area Detector System: The Xengen System, Version 2.0*, Genex Corporation, 16020 Industrial Drive, Gaithersburg, MD 20877 (software distributed by Siemens Analytical X-ray Instruments, 6300 Enterprise Lane, Madison, WI 53719).

Kenyon, G. L., & Hegeman, G. D. (1979) *Adv. Enzymol. Relat. Areas Mol. Biol. 50*, 325–360.

Landro, J. A., Kallarakal, A. T., Ransom, S. C., Gerlt, J. A., Kozarich, J. W., Neidhart, D. J., & Kenyon, G. L. (1991) *Biochemistry 30*, 9274–9281.

Neidhart, D. J., Howell, P. L., Petsko, G. A., Powers, V. M., Li, R., Kenyon, G. L., & Gerlt, J. A. (1991) *Biochemistry 30*, 6264–9273.

Nicolaou, K. C., Prasad, C. V. C., Hwang, C.-K., Duggan, M. E., & Veale, C. A. (1989) *J. Am. Chem. Soc. 111*, 5321–5330.

Powers, V. M., Koo, C. W., Kenyon, G. L., Gerlt, J. A., & Kozarich, J. W. (1991) *Biochemistry 30*, 9255–9263.

Sharp, T. R., Hegeman, G. D., & Kenyon, G. L. (1979) *Anal. Biochem. 94*, 329–334.

Tsou, A. Y., Ransom, S. C., Gerlt, J. A., Powers, V. M., & Kenyon, G. L. (1989) *Biochemistry 28*, 969–975.

Whitman, C. P., Craig, J. C., & Kenyon, G. L. (1985a) *Tetrahedron 41*, 1183–1192.

Whitman, C. P., Hegeman, G. D., Cleland, W. W., & Kenyon, G. L. (1985b) *Biochemistry 24*, 3936–3942.